

# A Magnetic Bald-Patch Flare in Solar Active Region 11117

Chaowei Jiang<sup>1,2</sup>, Xueshang Feng<sup>2,1</sup>, S. T. Wu<sup>3</sup> and Qiang Hu<sup>3</sup>

<sup>1</sup> HIT Institute of Space Science and Applied Technology, Shenzhen, 518055, China;  
*chaowei@hit.edu.cn*

<sup>2</sup> SIGMA Weather Group, State Key Laboratory for Space Weather, Center for Space Science and Applied Research, Chinese Academy of Sciences, Beijing 100190, China

<sup>3</sup> Center for Space Plasma and Aeronomic Research, The University of Alabama in Huntsville, Huntsville, AL 35899, USA Received XXX; accepted XXX

**Abstract** With SDO observations and a data-constrained MHD model, we identify a confined multi-ribbon flare occurred on 2010 October 25 in solar active region 11117 as a magnetic bald patch (BP) flare with strong evidences. From the photospheric magnetic field observed by SDO/HMI, we find there is indeed magnetic BPs on the PILs which match parts of the flare ribbons. From the 3D coronal magnetic field derived from a MHD relaxation model constrained by the vector magnetograms, we find strikingly good agreement of the BP separatrix surface (BPSS) footpoints with the flare ribbons, and the BPSS itself with the hot flaring loop system. Moreover, the triggering of the BP flare can be attributed to a small flux emergence under the lobe of the BPSS, and the relevant change of the coronal magnetic field through the flare is well reproduced by the pre-flare and post-flare MHD solutions, which match the corresponding pre and post-flare AIA observations, respectively. Our work contributes to the study of non-typical flares that constitute the majority of solar flares but cannot be explained by the standard flare model.

**Key words:** Sun: flares — Sun: corona — Magnetic fields — Magnetohydrodynamics (MHD) — Methods: numerical

## 1 INTRODUCTION

It is commonly believed that solar flares are explosive manifestation of magnetic energy release in the solar atmosphere by magnetic reconnection (Shibata & Magara 2011). The magnetic energy can be stored in the solar corona by means of magnetic flux emergence and/or energy injection by photospheric surface motions (shear/twist) from the sun's interior, and fast magnetic reconnection is the core process that release the stored energy. Depending on the specific coronal conditions, flares may be related with or without coronal mass ejections (CMEs). The eruptive flares, i.e., those accompanied with CMEs, are typically observed as with two flare ribbons roughly parallel along the main polarity inversion line (PIL) of magnetic field on the photosphere. These classical two-ribbon flares have been extensively studied, converging to a well-known standard flare model (i.e., the CSHKP flare model, Carmichael 1964; Sturrock 1966; Hirayama 1974; Kopp & Pneuman 1976), in which an eruptive magnetic flux rope (MFR) rises above the PIL, stretches the overlying field lines, produces a vertical current sheet underneath and triggers reconnection there, which results in the two-ribbon brightenings at the footprints of

the reconnecting field lines. Most of these flares occur in a common magnetic structure called sigmoidal active regions, which is manifestation of sheared bipolar field and favourable for formation of MFR.

On the other hand, there are numerous flares, either eruptive or confined, occur in a much more complicated manner than the classical two-ribbon flares. Flares associated with multiple ribbons of complex pattern are frequently reported in recent observations, such as quasi-circular ribbon flares (Masson et al. 2009; Wang & Liu 2012), three-ribbon flares (Wang et al. 2014), X-shaped flares (Li et al. 2016; Liu et al. 2016) and remote flare ribbons distinct from the eruptive core site (or the secondary ribbon, e.g., Zhang et al. 2014). These atypical flares appear to be more difficult to explain as no standard model exists. However, considering that a very big portion of the flares are atypical, it is necessary to emphasize on study of these complex flares (Dalmasse et al. 2014).

The variety of flare-ribbon pattern roots in the complexity of the underlying, invisible coronal field. For instance, the closed circular-like ribbon is found to be produced by a coronal magnetic null-point configuration (Masson et al. 2009; Wang & Liu 2012; Jiang et al. 2013). To generally understand how the flares occur, it is required to have the knowledge of where the reconnection might be triggered in a given configuration of the coronal field. Under typical coronal conditions, the plasma resistivity is extremely low and the magnetic field is frozen into the plasma almost everywhere in solar corona. As such, magnetic reconnection can only occur in certain places where the current form thin layers for the resistivity to be important to induce sufficient dissipation (Démoulin 2006, 2007). Such thin layers include the magnetic separatrices and more commonly, quasi-separatrix layers, across which the connectivity of field lines discontinues or changes abruptly, and consequently narrow, enhanced current sheets can easily form along there due to the photospheric driving motions (Priest & Forbes 2002; Titov et al. 2002; Longcope 2005).

Theoretical studies show that there are interesting places where coronal magnetic field lines become tangent to the photosphere at the PIL (e.g., Wolfson 1989; Low 1992; Titov et al. 1993). In such places, opposite to the normal case, the field line crosses the PIL from *negative* to *positive* polarity. These places are dubbed ‘bald patches’ (BPs) with the visual reference to a haircut with magnetic field lines being associated to hairs (Titov et al. 1993). Since the photosphere can be regarded as a line-tying boundary for the coronal field, a BP field line is thus very special because it is anchored at the BP in addition to its footpoints. As a result, the continuous set of BP field lines defines a separatrix surface (BPSS) of magnetic topology, across which the field-line linkage is discontinuous. This is rather important considering that BP is the only place that can define magnetic separatrices beside the case in which magnetic nulls are present in the corona. The field lines immediately above a BP are concave up (i.e., forming magnetic dips) and can hold material against solar gravity, which thus usually implies the existence of filament associated with BP (Titov & Démoulin 1999; Mackay et al. 2010). The criterion for the existence of BPs in the models of potential and linear force-free fields was given in detail by Titov et al. (1993).

For the case of BPSS, current sheets are very prone to be formed and thus reconnection can be triggered by shearing motions at the photosphere footpoints of the BP-separatrix field lines or pushing by flux emergence under the BP-separatrix lobe. By a 3D numerical MHD simulation driven by a bottom shearing velocity, Pariat et al. (2009) shows that current can form all along the curved BP separatrices where the reconnection can take place successively. There is another possibility in which vertical current sheet can be formed just above BP due to a converging and upward movement of the field lines from different lobes (see Figure 1 in Titov et al. 1993). By this pinching effect, the two BP lobes are brought into contact and lead to a vertical current sheet formed between the oppositely directed magnetic fields, which eventually reconnect. Besides, during the evolution of some magnetic configurations, BPs may be precursors of the emergence of a null point in the coronal field (Bungey et al. 1996), being again associated with reconnection processes. The BP separatrix also have a close relationship with MFR, which holds a central position in many flare/CME models (e.g., Forbes et al. 2006; Török & Kliem 2005; Kliem & Török 2006). During a MFR forming in the corona or emerging from below the photosphere, there might be a state when the MFR is bodily attached at the photosphere besides its two legs, and the BP separatrix is the interface between the MFR and the ambient field (Titov & Démoulin 1999). When viewed from above, this MFR-BPSS usually exhibits an S or inverse-S shape, and reconnection

there can produce a hot plasma in corresponding field lines, which can explain the observations of coronal sigmoids. Indeed, Jiang et al. (2014) recently found an almost coincidence of an EUV sigmoid in AR 11283 with the BPSS of a corresponding MFR reconstructed from HMI vector magnetogram.

In observation, BP was first related with flares by Aulanier et al. (1998), who found a close correspondence between the BP separatrices and the  $H\alpha$  and X-ray emissions in a very small flare (or sub-flare) in AR 7722, which was firstly interpreted as a so-called ‘BP flare’. Several observation studies also show that the reconnection triggered at BP can be correlated to eruptive flares. Delannée & Aulanier (1999) studied another example of BP-related flare and CME near AR 8100 and AR 8102, and suggested that the eruption is triggered by reconnection occurs in a vertical current sheet, which is formed above the BP due to the photospheric shearing motions and the line-tie condition at the BP (e.g., Titov et al. 1993). Wang et al. (2002) showed that in AR 8210 the emerging motion of a twist flux rope may drive a slow reconnection at a BP (manifesting as a flare), which removes the overlaying flux confining the flux rope to give way for the flux rope to expand and form a CME. Besides, BP are associated with a wider range of phenomena in the chromosphere and transition region, e.g., the transition region brightenings (Fletcher et al. 2001), in surge ejections and arch filament systems (Mandrini et al. 2002), and in Ellerman bombs, i.e., small-scale transient  $H\alpha$  brightenings (Pariat et al. 2004). All these phenomena are closely related with flux emergence, which is frequently observed in the solar atmosphere.

However, it should be noted that, probably due to the lack of the high-resolution vector magnetogram or the rather small scale of the related flare, the evidence for existence of BP in aforementioned examples of BP-flare was computed using an extrapolation of the photospheric field, particularly, the linear extrapolations (e.g., the potential, linear force-free or linear magnetohydrostatic models) based only on the line-of-sight component of the photospheric field. Such kind of evidence, obviously is very indirect and may be not reliable because of the limitation of the models, considering that the location of BPs can be deduced directly from vector magnetograms (with the  $180^\circ$  ambiguity resolved). Also it is very difficult to use a simple linear field model to recover the complex non-potential coronal structures, which is generally very nonlinear (e.g., Wiegmann 2008), although in some occasions, the basic topology of the magnetic field can be ‘sketched’ roughly using the linear models (Demoulin et al. 1997). To reconstruct the coronal field and capture the magnetic topology more precisely, it is necessary to use more realistic models, like the nonlinear force-free field (NLFFF) extrapolation or even the MHD model, with the photospheric vector field as input.

Now with the high-resolution and high-cadence vector magnetic field data and EUV observations from SDO, we have more opportunity to test the theory of BP-induced flare. Very recently, basing on a sophisticated topological analysis of NLFFF extrapolation from HMI vector magnetogram, Liu et al. (2014) suggested that magnetic reconnection at the BPSS may play an important role in producing an unorthodox X-class long-duration confined flare in AR 11339. In this paper we revisit a C-class confined flare event in AR 11117, which has been used for our validation of a CESE–MHD model for reconstructing coronal magnetic field based on the SDO/HMI vector magnetograms (Jiang et al. 2012). By analyzing the reconstructed magnetic field, we have preliminarily shown that there is a relation between this flare and a BP found on the vector magnetogram near the flare site and time. Here with the same modeling data we will give more concrete evidence of the correlation between the BP and the flare, and further show how the magnetic reconnection at the BP is activated and the corresponding change of the BP separatrices. The remainder of the paper is organized as follows. In Section 2 we describe the observations of the flare by SDO/AIA and in Section 3 we study the magnetic field on the photosphere and of the 3D topology, to provide the evidence of the BP-flare and show how the flare is triggered. We finally discuss the results and conclude in Section 4.

## 2 OBSERVATIONS

As shown in Figure 1, the studied flare occurred in AR 11117 on 2010 October 25, when the AR was crossing the central meridian of the solar disk with latitude of  $22^\circ\text{N}$ . On this day, AR 11117 is the largest one of the ARs on disk, and only one flare with class of C2.3 was recorded according to the GOES (Geostationary Operational Environmental Satellite) 1–8 Å light curve, which starts at 22:06 UT,

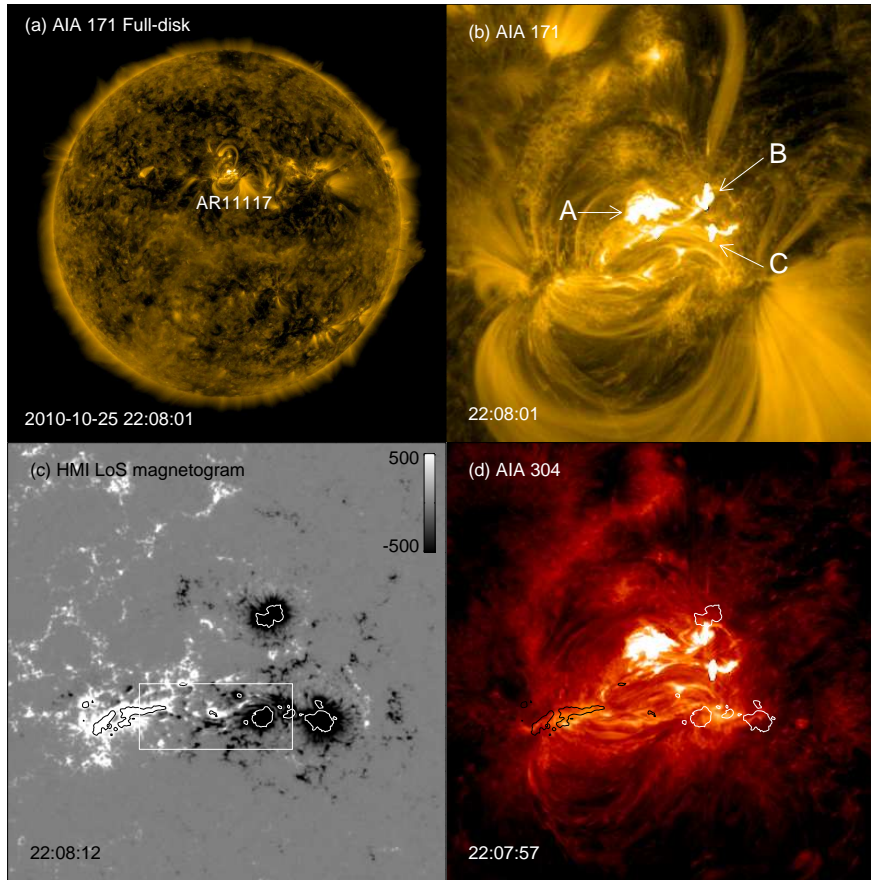


**Fig. 1** Location of the active region 11117 and the flare site. (a) Full-disk *SDO/AIA* 171 Å image with AR 11117 outlined by the white rectangle on the image. (b) Enlarged view of AR11117 in the full-disk image. The flare site with mainly three brightening kernels are labeled as A, B and C. (c) The HMI line-of-sight magnetogram for the same field-of-view of (b). Contour lines are plotted at  $\pm 1000$  G. The box region denotes a fast flux emergence site. (d) the AIA 304 Å image of the same region with the contour lines in (c) overlapped on the image.

peaks at 22:12 UT and ends at about 22:18 UT. The AR consists of two leading sunspots of negative polarity, one in the north and the other in the south, followed by an elongated positive polarity in the east, and fast magnetic flux emergence to the core of the region during the day (denoted by the box in Figure 1c). However, rather unexpectedly, the flare did not happen in the flux emerging site with strong magnetic shear, but in the intermediate region between the sunspots (especially much closer to the north sunspot, which is further away from the flux emergence site than the south one, see Figure 1b and d), where the field is relatively weak and no distinct magnetic shear is observed.

As recorded well by the AIA, the flaring process is confined in a rather low altitude without inducing major changes in the coronal loops or eruptions. Figure 2 gives the evolution of the flare site in detail with four EUV channels, the 171 Å for the corona and hot loops shown by 94 Å, the 304 Å for the upper chromosphere, and 1600 Å for the lower/middle chromosphere. It begins to brighten at 22:07 UT and ends at 22:15 UT. The flare brightening can be seen most clearly for several minutes around the time of 22:08 UT, which the Figure 1 is plotted for. We only roughly regard it consisting of three brightening

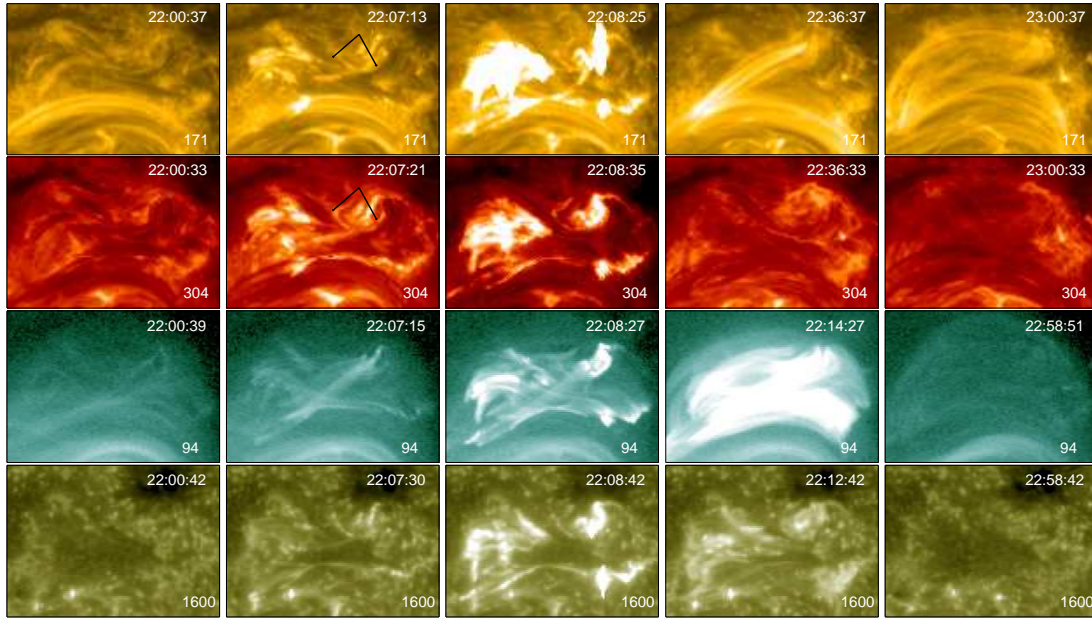


**Fig. 2** Coronal evolution through the flare observed by AIA in channels of 171 Å, 304 Å, 94 Å and 1600 Å.

kernels labeled as A, B and C on the AIA image (see Figure 1(b)), since these small patches are very close to each other and seem to be connected. The brightening patch at the east, A, is much bigger than the other two, B and C, at the west, indicating that more energy is delivered at A, and by carefully inspecting time-series of the AIA images (Figures 2) or time-lapse movies, it seems that the flare is first brightened at kernel A, where it might be activated or triggered, and then brightened at B and C, possibly because the energetic particles following the magnetic field lines to their footpoints. Note that actually the flare patch A consists of many even smaller patches by inspecting the 1600 Å, indicating multiple complex footpoints of the coronal magnetic field involved with reconnection.

As shown by the arrows on the AIA images of 171 Å and 304 Å in Figure 2, there appears to be a small curved dark feature overlying the flare kernels, indicating that field lines there exhibit some dips to support this filament-like material. This mini-filament sustained for hours before the onset of the flare, and disappeared after the flare (see the AIA images at time of 23:00 UT). As can be seen in AIA 171 Å, there is a new set of coronal loops expanding after the flare, just in the same location of the disappeared mini-filament.

### 3 STUDY OF THE MAGNETIC FIELD

In our previous work (Jiang et al. 2012; Jiang et al. 2016), we have developed a data-constrained CESE-MHD model to reconstruct the 3D coronal magnetic field. The MHD model, based on the space-time conservation-element and solution-element (CESE) scheme, is designed to focus on the magnetic-field evolution and to consider a simplified solar atmosphere in gravity with a small plasma  $\beta$ . Magnetic vector-field data derived from the observations at the photosphere is inputted directly to constrain the model. With regarding that for the studied event the coronal configuration changes are very limited and can be approximated by successive MHD equilibria, we have solved a time sequence of MHD equilibria basing on a set of vector magnetograms taken by HMI around the time of flare. The model and results have been given in details in (Jiang et al. 2012), which shows that the model successfully reproduces the basic structures of the 3D magnetic field, as supported by the good visual similarity between the field



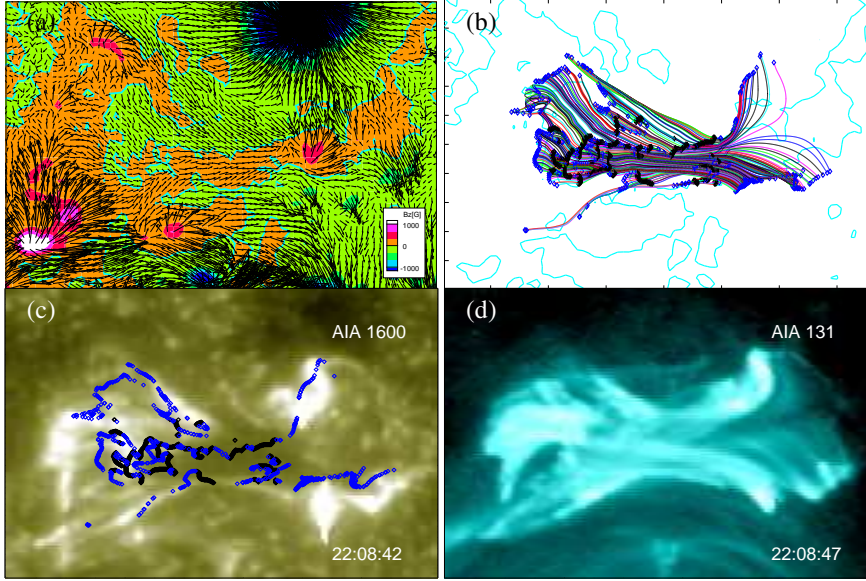


**Fig. 3** Spatial relation between the flare site and the BPSS. (a) Magnetic vector fields at the photosphere taken by HMI at 22:12 UT; (b) Magnetic field lines from the BPSS. The small diamond shapes in black denote the BPs, and those in blue for the footpoints of the BPSS field lines. The thick cyan line represents the photospheric magnetic PILs. (c) Flare brightening patches observed by AIA in 1600 Å, and the overlaid are the BPs and BPSS footpoints. (d) Hot flaring loops observed by AIA in 131 Å.

lines and the coronal loops observed by AIA. Here our analysis is confined to the magnetic topology and its change related with local region of the flare site.

Even before inspecting the coronal field, we find there is indeed BPs on the photosphere. With the vector magnetogram, one can identify BPs directly by searching for locations satisfying

$$B_z = 0 \text{ and } \mathbf{B} \cdot \nabla B_z > 0, \quad z = 0 \text{ (i.e., on the photosphere)}. \quad (1)$$

This equation characterizes portions of PILs where the horizontal field crosses from the negative to positive  $B_z$ . *SDO/HMI* has taken a sequence of vector magnetograms with cadence of 12 min. Here we select the magnetogram taken at 22:12 UT, see Figure 3 (a), which is mostly near the time of the flare. Locating of the BPs is carried out on a mesh refined by ten times from the original magnetogram using linear interpolation, and then we search for all the grid points fulfilling Equation (1). As shown in Figure 3 (c), the BP points are plotted as black diamond shapes overlaid on the AIA-1600 image (the grid coordinates are co-aligned with the the AIA image). Here it can be seen that the BP is clearly co-spatial with the flare location, mainly near flare patch A. The BPs mainly reside on the long PIL in the central region of the flare site (the thick cyan line on Figure 3 (b)), and there are some other small segments of BPs near this main PIL. On the main PIL, the BPs likely belong to a continuous long BP line, although they are disconnected frequently as derived from the observed vector field due to the noise of the magnetogram. One may worry about the reliability of the data since in this region the vector fields is relatively weak ( $\sim 200$  G), but considering that the directions of the magnetic vectors do not show the pattern of random noise, we can be confident with the existence of these BPs.

We note that no BP coincides with the flare patches B and C. Are this places related with the footpoints of the BPSS field lines? With the 3D coronal field model, we trace all the field lines passing through the BP points, which forms the BPSS, and locate the footpoints of all these BPSS field lines.

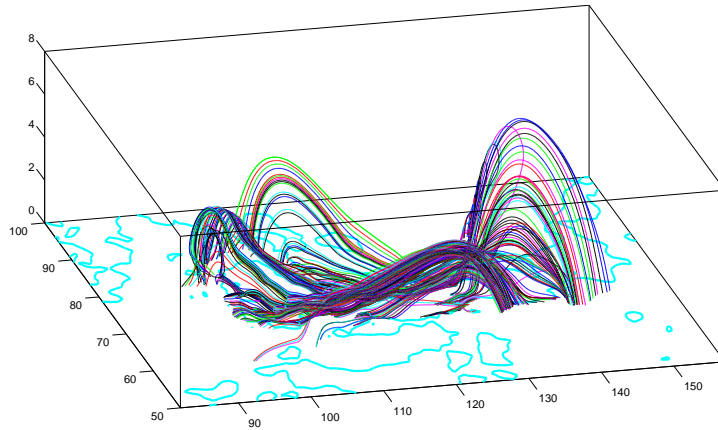


**Fig. 4** 3D view of the BPSS field lines as shown in Figure 3(b).

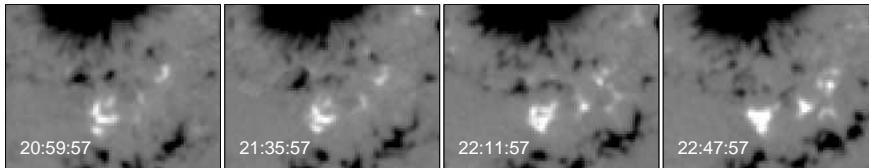


**Fig. 5** Time sequence of HMI magnetograms shows a small emerging positive polarity under the west lobe of the BPSS.

Figure 3 (b) shows all these BPSS field lines, and their footpoints are marked as blue diamonds, which are also overlaid on the AIA-1600 image. As we have conjectured, the western BPSS footpoints are co-spatial very well with the flare ribbon B and C, while the eastern footpoints coincides with flare patch A. A 3D view of the BPSS field lines is also shown in Figure 4, from which we can see that the apexes of the field lines are  $3 \sim 4$  Mm, thus the whole structure is very low. The field lines outline the topology of the separatrix surface which separates three different topological regions. The footpoints in the east are very near the BPs, thus their brightenings along with those from the BPs produce the big flare patch A that consists of many even-small flare patches. Moreover, there should be another separatrix surface (not shown here) at the west of the BPs, which divides the west part into two connectivity domains and results in two different sets of footpoints, thus produces the two flare patches B and C, respectively. Furthermore, comparing Figure 3 (b) with (d) shows that the shape of the BPSS is in good agreement with the hot flaring loop observed in AIA-131, strongly suggesting that reconnection occurs in this BPSS and heats the plasma in corresponding field lines to form the hot loops. Besides, the mini-filament as aforementioned (shown by arrows in Figure 2) might be supported at the dips of field lines just above the BP separatrix surface. The disappearance of this mini-filament after the flare seems to suggest that the dipped field lines are lift up by magnetic reconnection at the BPSS, which make the field lines detached from the photosphere at the BP, and consequently the dense plasma is drained off by gravity. However, there is also a possibility that the disappearance of the mini-filament is because it was heated to a higher temperature insensitive to AIA-171 and 304 passbands.

With the above study based on the field at the time of 22:12 UT, we have given a strong evidence that the flare is co-related with the BP, and the process of the event is suggested as following. Firstly magnetic

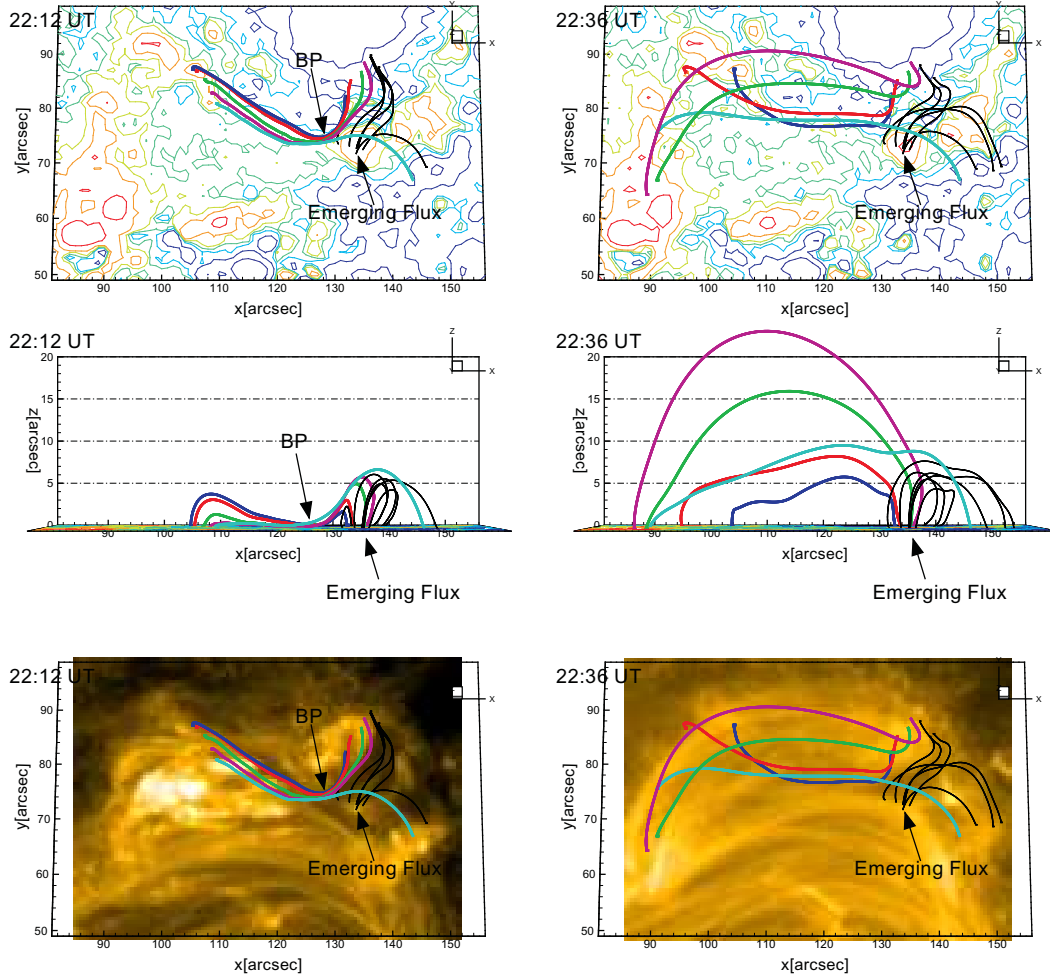


**Fig. 6** Magnetic configuration change from pre-flare state (left panels) to post-flare state (right panels). The magnetic field lines are shown in SDO view angle (top) and side view (middle), and overlaid on AIA-171 images (bottom). A group of BPSS field lines are shown in thick colored lines. Their footpoints in the west (the right side) are fixed for the pre-flare and post-flare field lines. A group of field lines from the emerging polarity are shown in black color. The contour lines represent photospheric magnetogram  $B_z$ , red for positive and blue for negative.

reconnection is activated at the BP, then the accelerated particles there traced the field lines near the BP-separatrix and produced flare ribbons, and the field lines that attached the photosphere at the BP before the flare are lift up by the reconnection and expand upward, manifesting by the emergence of the post-flare loops and the disappearance of the mini-filament. Such and similar processes can usually be related with flux emergence, which can trigger reconnection in the BPSS, for example in the formation of active region (Pariat et al. 2004) and in the surges and arch filament systems (Mandrini et al. 2002). In the present event, by inspecting the photospheric field evolution, we find that there is indeed an emergence of a small positive polarity under the west lobe of the BPSS, see Figure 5. With the evolution of the reconstructed magnetic field we are able to illustrate how the BPSS field lines evolves through



the flare. The left panels of Figure 6 show several of BPSS field lines (the colored thick lines) before the flare, while the right panels show their post-flare configuration. Under the west lobe of the BPSS, the emerging positive polarity is shown with a set of field lines (the black thick lines). The field lines rooted in the emerging flux expand upward (as comparing the post-flare state with the pre-flare state) and push the overlaying BPSS, which continuously increases electric currents in the BPSS and free energy to the system. When the current sheet is enhanced enough for resistivity to be important, magnetic reconnection sets in at the BPSS, and the field lines attached at the BP by the photosphere plasma are lift up, expand as they relax, forming the post-flare loops. The field lines might also undergo slipping reconnection as they expand, with the footpoints not necessarily being in the same pre-flare locations. In the bottom panels, the field lines are overplotted on the AIA-171 images, which demonstrates a nice agreement of the model field lines with the coronal loops.

#### 4 CONCLUSIONS

In this study, we analyzed a C2.3 confined flare in AR 11117 with SDO observation and data-constrained MHD models. The flare is a non-standard one consisting of multiple ribbons, and it occurs in a region between the AR sunspots where the magnetic field is relatively weak and no distinct magnetic shear is observed, although the AR contains a typical fast-emerging and strong-field site with significantly sheared PIL. With strong evidences, we concluded that this flare is triggered by magnetic reconnection in a BPSS and can be identified as a BP flare:

1. By direct inspecting the photospheric magnetic vector field measured by SDO/HMI, we find there are BPs on the PILs matching parts of the flare ribbons.
2. From the 3D coronal magnetic field derived from the MHD model constrained by the vector magnetograms, we find strikingly good agreement of the BPSS footpoints with the flare ribbons, and the BPSS itself with the hot flaring loop system.
3. Moreover, the triggering of the BP flare can be attributed to a small flux emergence under the lobe of the BPSS, and the relevant change of the coronal magnetic field is well reproduced by the pre and post-flare MHD solutions which matches the corresponding pre and post-flare AIA observations. The flux emergence under the lobe of the BPSS triggers reconnection at the BP, making the pre-flare field lines that attached the photosphere at the BP relax and expand upward and form the post-flare loops.

Our work contributes to the study of non-typical flares that constitute the majority of solar flares but cannot be explained by the standard flare model. It is also worth noting that here the flare scenario is shown by MHD results constrained by observation data, and such data-constrained or even data-driven MHD modeling the evolution of coronal magnetic field is becoming an new important approach for gaining a comprehensive understanding of the physical nature of non-typical flares (Jiang et al. 2016).

**Acknowledgements** This work is jointly supported by National Natural Science Foundation of China (41531073, 41374176, 41574170, 41231068, and 41574171) and the Specialized Research Fund for State Key Laboratories. Data from observations are courtesy of NASA SDO/AIA and the HMI science teams

#### References

- Aulanier, G., Démoulin, P., Schmieder, B., Fang, C., & Tang, Y. H. 1998, *Sol. Phys.*, 183, 369  
 Bungey, T. N., Titov, V. S., & Priest, E. R. 1996, *A&A*, 308, 233  
 Carmichael, H. 1964, *NASA Special Publication*, 50, 451  
 Dalmasse, K., Chandra, R., Schmieder, B., & Aulanier, G. 2014, arXiv preprint arXiv:1410.8194  
 Delannée, C., & Aulanier, G. 1999, *Sol. Phys.*, 190, 107  
 Démoulin, P. 2006, *Advances in Space Research*, 37, 1269  
 Démoulin, P. 2007, *Advances in Space Research*, 39, 1367

- Demoulin, P., Bagala, L. G., Mandrini, C. H., Henoux, J. C., & Rovira, M. G. 1997, *A&A*, 325, 305
- Fletcher, L., López Fuentes, M. C., Mandrini, C. H., et al. 2001, *Sol. Phys.*, 203, 255
- Forbes, T. G., Linker, J. A., Chen, J., et al. 2006, *Space Sci. Rev.*, 123, 251
- Hirayama, T. 1974, *Sol. Phys.*, 34, 323
- Jiang, C., Feng, X., Wu, S. T., & Hu, Q. 2012, *ApJ*, 759, 85
- Jiang, C., Wu, S. T., & Feng, X. 2016, *Frontiers in Astronomy and Space Sciences*, 3, 16
- Jiang, C., Wu, S. T., Feng, X., & Hu, Q. 2014, *ApJ*, 786, L16
- Jiang, C. W., Feng, X. S., Wu, S. T., & Hu, Q. 2013, *ApJ*, 771, L30
- Jiang, C. W., Wu, S. T., Feng, X. S., & Hu, Q. 2016, *Nature Comm.*, 7, 11522
- Kliem, B., & Török, T. 2006, *Physical Review Letters*, 96, 255002
- Kopp, R. A., & Pneuman, G. W. 1976, *Sol. Phys.*, 50, 85
- Li, Y., Qiu, J., Longcope, D. W., Ding, M. D., & Yang, K. 2016, *The Astrophysical Journal*, 823
- Liu, R., Chen, J., Wang, Y., & Liu, K. 2016, *Scientific Reports*, 6, 34021
- Liu, R., Titov, V. S., Gou, T., et al. 2014, *ApJ*, 790, 8
- Longcope, D. W. 2005, *Living Reviews in Solar Physics*, 2, 7
- Low, B. C. 1992, *A&A*, 253, 311
- Mackay, D. H., Karpen, J. T., Ballester, J. L., Schmieder, B., & Aulanier, G. 2010, *Space Sci. Rev.*, 151, 333
- Mandrini, C. H., Démoulin, P., Schmieder, B., Deng, Y. Y., & Rudawy, P. 2002, *A&A*, 391, 317
- Masson, S., Pariat, E., Aulanier, G., & Schrijver, C. J. 2009, *ApJ*, 700, 559
- Pariat, E., Aulanier, G., Schmieder, B., et al. 2004, *ApJ*, 614, 1099
- Pariat, E., Masson, S., & Aulanier, G. 2009, *ApJ*, 701, 1911
- Priest, E. R., & Forbes, T. G. 2002, *A&A Rev.*, 10, 313
- Shibata, K., & Magara, T. 2011, *Living Reviews in Solar Physics*, 8, 6
- Sturrock, P. A. 1966, *Nature*, 211, 695
- Titov, V. S., & Démoulin, P. 1999, *A&A*, 351, 707
- Titov, V. S., Hornig, G., & Démoulin, P. 2002, *J. Geophys. Res.*, 107, 1164
- Titov, V. S., Priest, E. R., & Demoulin, P. 1993, *A&A*, 276, 564
- Török, T., & Kliem, B. 2005, *ApJ*, 630, L97
- Wang, H., & Liu, C. 2012, *ApJ*, 760, 101
- Wang, H., Liu, C., Deng, N., et al. 2014, *ApJ*, 781, L23
- Wang, T., Yan, Y., Wang, J., Kurokawa, H., & Shibata, K. 2002, *ApJ*, 572, 580
- Wiegmann, T. 2008, *Journal of Geophysical Research (Space Physics)*, 113, A03S02
- Wolfson, R. 1989, *ApJ*, 344, 471
- Zhang, J., Li, T., & Yang, S. 2014, *The Astrophysical Journal Letters*, 782, L27